RSC Advances

ROYAL SOCIETY OF CHEMISTRY

www.rsc.org/advances

The effect of the electrolyte additive of hexamethylenetetramine on the electrochemical behaviors of the Mg-11Li-3.5Al-2Zn-1.5Re-0.5Zr electrode

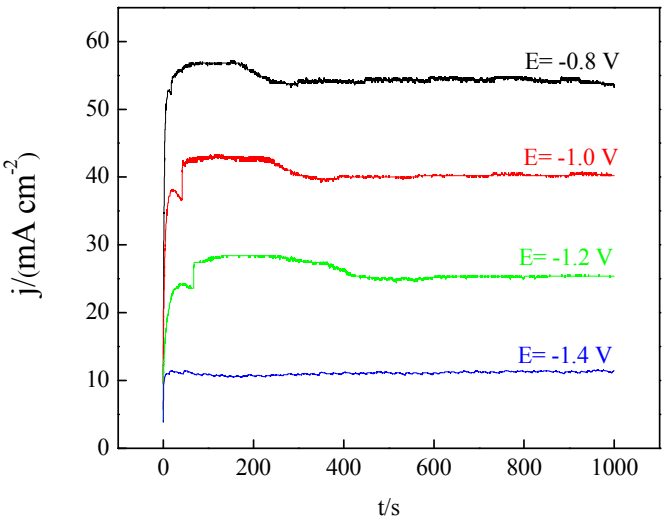

The current-time curves measured at different potentials for the Mg-11Li-3.5Al-2Zn-1.5Re-0.5Zr electrode in 0.7 mol L^{-1} NaCl solution containing concentrations of 0.10 mmol L^{-1} $C_6H_{12}N_4$.

The effect of the electrolyte additive of hexamethylenetetramine on the electrochemical behaviors of the Mg-11Li-3.5Al-2Zn-1.5Re-0.5Zr electrode

Yan-zhuo Lv[1,] *, *Yan-feng Li, Li Wang, Dian-xue Cao, Gui-ling Wang，Jing Feng, Yueming Ren, Milin Zhang*

Key Laboratory of Superlight Material and Surface Technology of Ministry of Education, College of Material Science and Chemical Engineering, Harbin Engineering University, Harbin 150001, P. R. China

*To whom all the correspondence should be addressed. E-mail: lvyanzhuo@hrbeu.edu.cn

Abstract

The electrochemical performances of the Mg-11Li-3.5Al-2Zn-1.5Re-0.5Zr electrode in 0.7 mol L^{-1} NaCl solution containing different concentrations of hexamethylenetetramine ($C_6H_{12}N_4$) as the electrolyte additive are investigated by means of potentiodynamic polarization, potentiostatic current-time and electrochemical impedance spectra measurements as well as by scanning electron microscopy examination (SEM). The potentiodynamic polarization curves show that the corrosion potential of the electrode increases in the following order with the concentrations of $C_6H_{12}N_4$: 0.10 mmol L^{-1} < 0.05 mmol L^{-1} < 2.00 mmol L^{-1} < 0.50 mmol L^{-1} < 0.80 mmol L^{-1}< 1.00 mmol L^{-1} < 0.00 mmol L^{-1}. The potentiostatic current-time curves

indicate that the oxidation current density of the electrode in 0.7 mol L^{-1} NaCl solution containing 0.10 mmol L^{-1} $C_6H_{12}N_4$ is the largest among the electrolyte solution studied, and the polarization resistance of the Mg-11Li-3.5Al-2Zn-1.5Re-0.5Zr electrode in 0.7 mol L^{-1} NaCl solution containing 0.10 mmol L^{-1} $C_6H_{12}N_4$ is smaller than that in 0.7 mol L^{-1} NaCl solution. The scanning electron microscopy studies indicate that the presence of $C_6H_{12}N_4$ in 0.7 mol L^{-1} NaCl solution can loosen the oxidation products and promote its coming off, consequently enhance the discharging performances of the Mg-11Li-3.5Al-2Zn-1.5Re-0.5Zr electrode.

1. Introduction

Magnesium-lithium-based alloy is one of the most potential anode materials because of its high energy density, high electrode potential, low density and environmental friendliness [1-4]. The electrochemical behaviors of the magnesium-based alloy as the anode materials of magnesium-hydrogen peroxide (Mg-H_2O_2) semi-fuel cells have been studied [5-9]. Sivashanmugam et Medeiros et al. [1] investigated the performances of Mg-H_2O_2 semi-fuel cells with magnesium alloy AZ61 as anode, carbon fiber supported Pd-Ir as cathode catalyst, H_2O_2 + H_2SO_4 as cathode-active components, seawater as electrolyte, and Nafion -115 as membrane. The practical cell voltage is above -1.7 V at 25 mA cm^{-2} with magnesium and hydrogen peroxide efficiencies ranging from 77% to 86% and specific energies ranging from 500 to 520 Wh kg^{-1} based on the weights of the magnesium anode, hydrogen peroxide, and acid consumed during discharge. However, the magnesium-based alloys as the anode

materials also show some disadvantages, such as parasitic corrosion reactions and self-discharge, which limits its extensive utilization in the electrochemical fields. Therefore, the electrochemical behaviors of magnesium and its alloys are still a significant research field and need to be widely investigated in various environments.

In order to enhance the performances of the magnesium-based alloy anodes, some alloying elements were added into the alloys, such as lithium, aluminum, zinc, silver, silicon, cadmium, and rare earth (RE) elements [10]. Cao et al. [11-13] reported that magnesium-lithium-based alloys exhibited high electro-oxidation activity in 0.7 mol L^{-1} NaCl solution. They found that Ce can enhance both the discharge activity and utilization efficiency. Sn mainly improves the discharge current. Our group [14-16] reported the electrochemical behaviors of the Mg-Li-Al-Ce, Mg-Li-Al-Ce-Y, Mg-8Li-0.5Y, Mg-8Li-1Y, Mg-8Li-3Al-0.5Zn and Mg-8Li-3Al-1.0Zn alloys in 0.7 mol L^{-1} NaCl solution. It was found that Y can change the alloy structure or assist the formation of an easy-peel off layer on the surface of the alloys. The content of Zn in the alloys affected the performances of the alloys and the Zn content of 0.5 wt. % is better than 1 wt. %. Modifying the Y content can alter the performances of the Mg-Li-Y alloy as the anode material of Mg-H_2O_2 semi-fuel cells. The Mg-8Li-1Y electrode has higher discharge activity and peak power density compared with that of Mg-8Li-0.5Y electrode. Ma et al. [17] investigated the corrosion behaviors and the discharge performances of the Mg, AZ31 and Mg-Li-Al-Ce electrodes in 3.5 wt. % NaCl solution. It was found that the Mg-Li-Al-Ce electrode has the higher electrochemical activity and lower self-corrosion rate than that of Mg and AZ31

electrodes. At a current density of 2.5 mA cm^{-2}, the operate voltage of the Mg-Li-Al-Ce anode is 1.272 V, the specific discharge capacity is 2076 mAh g^{-1}, and the anodic utilization efficiency is 85.2%. Modifying the electrolyte by including additives is also investigated to improve the performances of the magnesium-lithium-based alloy anodes. Cao et al. [11] investigated the effects of the electrolyte additive of Ga_2O_3 on the discharge performances of the Mg, Mg-Li, Mg-Li-Al and Mg-Li-Al-Ce electrodes. It has been found that Ga_2O_3 electrolyte additive can enhance the discharge currents and utilization efficiencies of the electrode. The utilization efficiency of the quaternary Mg-Li-Al-Ce electrode reaches to as high as around 82% and 88% in the absence and presence of gallium oxide additive, respectively.

In this study, the effect of different concentrations (0.00 mmol L^{-1}, 0.05 mmol L^{-1}, 0.10 mmol L^{-1}, 0.50 mmol L^{-1}, 0.80 mmol L^{-1}, 1.00 mmol L^{-1}, 2.00 mmol L^{-1}) of $C_6H_{12}N_4$ as the electrolyte additive on the electrochemical performances of the Mg-11Li-3.5Al-2Zn-1.5Re-0.5Zr electrode in 0.7 mol L^{-1} NaCl solution were investigated.

2. Experimental

2.1 Preparation of the Mg-11Li-3.5Al-2Zn-1.5Re-0.5Zr alloy

The alloy in this study was prepared by induction melting method. The materials used in this work were commercial pure ingots magnesium (99.99%), lithium (99.99%), aluminum (99.99%), zinc (99.99%), rhenium (99.99%), zirconium (99.99%). As reported [14, 16, 18], the ingots were loaded in a graphite crucible and were melted under

the protection of an atmosphere of pure argon, then the melt was slowly cast into a 125 mm × 37 mm steel mold to obtain as-cast alloy. The nominal compositions of the alloys are given in Table 1.

2.2 Electrochemical measurements

A specifically designed home-made three-electrode electrochemical cell [18] was used. The cell was equipped with a platinum counter electrode, a saturated calomel reference electrode (SCE), and the Mg-11Li-3.5Al-2Zn-1.5Re-0.5Zr alloy working electrode. The alloy ingots were machined to 15 mm × 15 mm × 5 mm. Prior to each experiment, the sample was successively polished with SiC abrasive papers to 600 grit, 1000 grit and 2000 grit, washed with deoxygenated ultrapure water (Milli-Q), degreased with acetone and rinsed with deoxygenated ultrapure water again.

Electrochemical experiments were carried out in 0.7 mol L^{-1} NaCl solution with different concentrations of $C_6H_{12}N_4$ at room temperature. The solution was purged with N_2 gas for 15 minutes before measurements in order to remove the dissolved O_2. The exposure area of the alloy electrode is 0.5 cm^2, which was used to calculate the current density. Electrochemical measurement techniques included potentiodynamic polarization (10 mV s^{-1}, -2.2 V to -0.8 V), potentiostatic oxidation (15 min, at -0.8 V, -1.0 V, -1.2 V and -1.4 V), electrochemical impedance spectroscopy (0.1-10^5 Hz, 5 mV, under open circuit potential).

2.3 Characterizations of the alloy

The surface morphology of the Mg-11Li-3.5Al-2Zn-1.5Re-0.5Zr electrode was measured with scanning electron microscopy (SEM, JEOL JSM-6480) after the test of

the potentiostatic oxidation. The alloy composition was determined using the energy dispersive spectrometer (EDS) with Vantage Digital Acquisition Engine (Thermo Noran, USA).

3. Results and discussion

3.1. The effect of $C_6H_{12}N_4$ as the electrolyte additive on the potentiodynamic polarization curves of the Mg-11Li-3.5Al-2Zn-1.5Re-0.5Zr electrode

Fig. 1 depicts the potentiodynamic polarization curves of the Mg-11Li-3.5Al-2Zn-1.5Re-0.5Zr electrode in 0.7 mol L^{-1} NaCl solution containing different concentrations of $C_6H_{12}N_4$ (0.00 mmol L^{-1}; 0.05 mmol L^{-1}; 0.10 mmol L^{-1}; 0.50 mmol L^{-1}; 0.80 mmol L^{-1}; 1.00 mmol L^{-1}; 2.00 mmol L^{-1}). The corrosion potential of the Mg-11Li-3.5Al-2Zn-1.5Re-0.5Zr electrode is slightly more negative in the 0.7 mol L^{-1} NaCl solution with $C_6H_{12}N_4$ than that without $C_6H_{12}N_4$. The potentiodynamic polarization measurements show that the corrosion potential of the Mg-11Li-3.5Al-2Zn-1.5Re-0.5Zr electrode reduces in the following order according to the concentrations of $C_6H_{12}N_4$: 0.00 mmol L^{-1} (-1.521 V) > 1.00 mmol L^{-1} (-1.524 V) > 0.80 mmol L^{-1} (-1.534 V) > 0.50 mmol L^{-1} (-1.543 V) > 2.00 mmol L^{-1} (-1.557 V) > 0.05 mmol L^{-1} (-1.585 V) > 0.10 mmol L^{-1} (-1.596 V). These results indicate that the electrochemical activity of the electrode was improved, but it is not a simple incremental relationship according to the increase of its concentration. When the concentration of $C_6H_{12}N_4$ is 0.10 mmol L^{-1}, the corrosion potential of the Mg-11Li-3.5Al-2Zn-1.5Re-0.5Zr electrode is the most negative and its electrochemical activity is the best. 0.1 mmol L^{-1} $C_6H_{12}N_4$ shows the highest activity probably because

that certain optimal interaction effect takes place between $C_6H_{12}N_4$ and the oxidation products of the electrode and the optimal interaction effect takes place between $C_6H_{12}N_4$ and the electrode. 0.1 mmol L^{-1} $C_6H_{12}N_4$ may best facilitate the dissolution and then exfoliation of the oxidation product from electrode surface, thus it is difficult for oxidation product to form compact protective film, which means the magnesium-lithium alloy anode is in continuous active dissolution condition. The foregoing reactions facilitate the electrode to keep larger available discharging surface area, that is to say the increase of the active points of the electrochemical reaction, therefore the electro-oxidation activity in the electrolyte solution with 0.1 mmol L^{-1} $C_6H_{12}N_4$ is best improved. And 0.1 mmol L^{-1} $C_6H_{12}N_4$ in the electrolyte solution may also have some optimal promotion effect on the electrochemical reaction of the electrode. Its existence may decrease the activation energy of the electrode reaction and accelerate the reaction rate to the most degree. Thus, 0.1 mmol L^{-1} $C_6H_{12}N_4$ shows the highest activity.

3.2. The effect of $C_6H_{12}N_4$ as the electrolyte additive on the potentiostatic current-time curves of the Mg-11Li-3.5Al-2Zn-1.5Re-0.5Zr electrode

Figs. 2-5 depicts the potentiostatic oxidation curves of the Mg-11Li-3.5Al-2Zn-1.5Re-0.5Zr electrode measured at the constant potentials of -0.8 V, -1.0 V, -1.2 V, -1.4 V in 0.7 mol L^{-1} NaCl solution with different concentrations of $C_6H_{12}N_4$ (0.00 mmol L^{-1}, 0.05 mmol L^{-1}, 0.10 mmol L^{-1}, 0.50 mmol L^{-1}, 0.80 mmol L^{-1}, 1.00 mmol L^{-1}, 2.00 mmol L^{-1}), which is carried out to evaluate the discharge performances of the Mg-11Li-3.5Al-2Zn-1.5Re-0.5Zr electrode. It can be seen from

the diagrams that the potentiostatic oxidation curves have the similar shape under the four different potentials. The anodic current increased rapidly due to the double layer charging in the initial stage and then reached to an approximate constant value, and the oxidation current density of the Mg-11Li-3.5Al-2Zn-1.5Re-0.5Zr electrode is the highest at the concentration of the additive of 0.10 mmol L^{-1}. At the constant potential of -0.8 V, the oxidation current density of the electrode in 0.7 mol L^{-1} NaCl solution with 0.10 mmol L^{-1} $C_6H_{12}N_4$ (52.99 mA cm^{-2}) is 30.95% higher than that in 0.7 mol L^{-1} NaCl solution (40.50 mA cm^{-2}); at the constant potential of -1.4 V, the oxidation current density of the electrode in 0.7 mol L^{-1} NaCl solution with 0.10 mmol L^{-1} $C_6H_{12}N_4$ (11.02 mA cm^{-2}) % is 134.04% higher than that in 0.7 mol L^{-1} NaCl solution (4.56 mA cm^{-2}). Fig. 3 shows that at the constant potential of -1.0 V, the oxidation current density of the electrode increases when the concentration of $C_6H_{12}N_4$ is 0.10 mmol L^{-1}, 0.50 mmol L^{-1} and 0.80 mmol L^{-1}, and the oxidation current density of the electrode is 41.90 mA cm^{-2} with the concentration of 0.10 mmol L^{-1} $C_6H_{12}N_4$, which is 21.74% higher than that in 0.7 mol L^{-1} NaCl solution (34.70 mA cm^{-2}). Fig. 4 shows that at the constant potential of -1.2 V, the oxidation current density of the electrode was increased to 26.10 mA cm^{-2} when the concentration of $C_6H_{12}N_4$ was 0.10 mmol L^{-1}, which is 11.59% higher than that in 0.7 mol L^{-1} NaCl solution (23.45 mA cm^{-2}). The reason for different behaviors of the electrode in electrolyte solution containing $C_6H_{12}N_4$ higher than 0.1 mmol L^{-1} at potential range of -0.8 to -1.4 V (figures 2-5) is probably resulting from the electrode process. As is known to all that electrode process is complicated and it is mainly controlled by electrochemical polarization and

concentration polarization. The changes of surface condition of the electrode, such as adsorption/desorption of active substance on the electrode/electrolyte interface as well as formation and dissolution of oxide film, directly influence the electrochemical reaction rate. According to current research results, the reason for this phenomenon could be explained as follows: size and thickness of the oxide film varying with different concentrations of additive act on the electrode surface, and correspondingly change the discharging performances of the electrode at different degree.

3.3. The effect of $C_6H_{12}N_4$ as the electrolyte additive on the impedance spectra of the Mg-11Li-3.5Al-2Zn-1.5Re-0.5Zr electrode

The complex impedance technique was used as a basis for a comparative study to show the discharge behavior of the Mg-11Li-3.5Al-2Zn-1.5Re-0.5Zr electrode at the open circuit potential in 0.7 mol L^{-1} NaCl electrolyte solution with $C_6H_{12}N_4$ (0.00 mmol L^{-1}, 0.10 mmol L^{-1}). The Nyquist plots are shown in Fig. 6. The single frequency capacitive arc is considered to be caused by charge transfer [19, 20] and the diameter of the semicircle represents the polarization resistance Rp. The Rp of the Mg-11Li-3.5Al-2Zn-1.5Re-0.5Zr electrode in 0.7 mol L^{-1} NaCl solution containing 0.10 mmol L^{-1} $C_6H_{12}N_4$ (ca.138 Ω cm^{-2}) is smaller than that of Mg-11Li-3.5Al-2Zn-1.5Re-0.5Zr electrode in 0.7 mol L^{-1} NaCl solution (ca.281 Ω cm^{-2}). This indicates that the charge transfer activity of the Mg-11Li-3.5Al-2Zn-1.5Re-0.5Zr electrode in 0.7 mol L^{-1} NaCl solution containing 0.10 mmol L^{-1} $C_6H_{12}N_4$ is higher than that of Mg-11Li-3.5Al-2Zn-1.5Re-0.5Zr electrode in 0.7 mol L^{-1} NaCl solution. Therefore, the electrolyte additive of $C_6H_{12}N_4$

affected the electrochemical activity of the alloy electrode obviously. This might due to the surface of the electrode is difficult to form a passive layer in the electrolyte solution containing 0.10 mmol L^{-1} $C_6H_{12}N_4$ during the discharging state. Thus, the liquid electrolyte is easier to contact with the electrode, leading to the larger corrosion current and the better electro-oxidation activity. $C_6H_{12}N_4$ may change the structure of the alloy or assist the formation of an easy-peel-off layer on the alloy surface. These results are in good agreement with the results obtained from potentiodynamic polarization curves (Fig. 1) and potentiostatic current-time curves (Figs. 2, 3, 4 and 5).

3.4. The effect of $C_6H_{12}N_4$ as the electrolyte additive on the morphology of the Mg-11Li-3.5Al-2Zn-1.5Re-0.5Zr electrode

Fig. 7a, b and c show the SEM micrographs of the Mg-11Li-3.5Al-2Zn-1.5Re-0.5Zr alloy after the samples discharged for 15 min at -1.0 V in 0.7 mol L^{-1} NaCl solution with different concentrations of $C_6H_{12}N_4$(0.00 mmol L^{-1}, 0.10 mmol L^{-1}, 1.00 mmol L^{-1}), respectively. Obviously, the discharge products of the Mg-11Li-3.5Al-2Zn-1.5Re-0.5Zr electrodes existed in different forms. Fig. 7a demonstrated that the discharge products attached on the Mg-11Li-3.5Al-2Zn-1.5Re-0.5Zr alloy surface after discharging in 0.7 mol L^{-1} NaCl solution present as micro-clumps and wires. Fig.7c show the surface morphology of the electrode in 0.7 mol L^{-1} NaCl solution with 1.00 mmol L^{-1} $C_6H_{12}N_4$, which shows the relatively dense oxide surface. Fig.7b indicated that the oxidation products of the Mg-11Li-3.5Al-2Zn-1.5Re-0.5Zr alloy after discharging in 0.7 mol L^{-1} NaCl solution containing 0.10 mmol L^{-1} $C_6H_{12}N_4$ formed thick and large micro-blocks on the surface.

From Fig.7b, the deeper and larger channels on the surface of the Mg-11Li-3.5Al-2Zn-1.5Re-0.5Zr electrode allow the electrolyte to penetrate through more easily and also allow the oxidation products to come off more easily. Consequently, the Mg-11Li-3.5Al-2Zn-1.5Re-0.5Zr electrode retains larger reaction surface area in the presence of $C_6H_{12}N_4$ than that in the absence of $C_6H_{12}N_4$, so the reaction rate is increased and it is beneficial for the improvement of the current density. On the whole, the electrochemical oxidation activity of the Mg-11Li-3.5Al-2Zn-1.5Re-0.5Zr electrode was improved after the electrolyte additive of $C_6H_{12}N_4$ with the concentration of 0.10 mmol L^{-1} was added into 0.7 mol L^{-1} NaCl solution, which is consistent with the results obtained from the potentiostatic current-time curves (Figs. 2, 3, 4 and 5).

4. Conclusions

In this article, the following conclusions can be obtained by the analysis of the corrosion potential, the oxidation current density, the polarization resistance, the surface morphologies of the electrode:

(1) The concentrations of the electrolyte additive of $C_6H_{12}N_4$ can affect the electrochemical performances of the Mg-11Li-3.5Al-2Zn-1.5Re-0.5Zr electrode in 0.7 mol L^{-1} NaCl solution.

(2) The corrosion potential of the Mg-11Li-3.5Al-2Zn-1.5Re-0.5Zr electrode is shifted to the negative direction when $C_6H_{12}N_4$ was added into 0.7 mol L^{-1} NaCl solution, and the most negative potential was found that at the concentration of the additive is 0.10 mmol L^{-1}.

(3) The current density of the Mg-11Li-3.5Al-2Zn-1.5Re-0.5Zr electrode is the biggest when 0.10 mmol L^{-1} $C_6H_{12}N_4$ is added into 0.7 mol L^{-1} NaCl solution.

(4) Under open circuit potential, the polarization resistance of the Mg-11Li-3.5Al-2Zn-1.5Re-0.5Zr electrode in 0.7 mol L^{-1} NaCl solution containing 0.10 mmol L^{-1} $C_6H_{12}N_4$ is ca.138 Ω cm^{-2} which is smaller than that in 0.7 mol L^{-1} NaCl solution (ca.281 Ω cm^{-2}). And the electrode surface forms larger and deeper crackles, the product is not easy to accumulate on the electrode surface, which will result in the deeper penetration of the electrolyte, and it is also helpful to increase the electrochemical oxidation current density of the Mg-11Li-3.5Al-2Zn-1.5Re-0.5Zr electrode.

Acknowledgements

This work was financially supported by the National Natural Science Foundation of China (21203040, 21301038, 51108111), the Natural Science Foundation of Heilongjiang Province of China (B201201), and the Fundamental Research Funds for the Central Universities (HEUCF201403018).

References

1. M G Medeiros, R R Bessette, C M Deschenes, C J Patrissi, L G Carreiro, S P Tucker, D W Atwater, J. Power Sources, 2004, **136**, 226-231.

2. M. C. Lin, C. Y. Tsai, J. Y. Uan, Corros. Sci. 2009, **51**, 2463-2472.

3. R. R. Bessette, M. G. Medeiros, C. J. Patrissi, C. M. Deschenes, C. N. LaFratta, J. Power Sources, 2001, **96**, 240-244.

4. D. J. Brodrecht, J. J. Rusek, J, Applied Energy, 2003, **74**, 113-124.

5. R. R. Bessette, J. M. Cichon, D. W. Dischert, E. G. Dow, J. Power Sources, 1999, **80**, 248-253.

6. W. Q. Yang, S. H. Yang, W. Sun, G. Q. Sun, Q. Xin, J. Power Sources, 2006, **160**, 1420-1424.

7. D. J. Brodrecht, J. J. Rusek, Appl. Energy, 2003, **74**, 113-124.

8. W. Q. Yang, S. H. Yang, W. Sun, G. Q. Sun, Q. Xin, J. Power Sources, 2006, **52**, 9-14.

9. O. Hasvold, N. J. Storkersen, S.Forseth, T. Lian, J. Power Sources, 2006, **162**, 935-942.

10 G. Liang, J. Alloys Compd, 2004, **370**, 123-128.

11. D. X. Cao, L. Wu, G. L. Wang, Y. Z. Lv, J. Power Sources, 2008, **183**, 799-804.

12. D. X. Cao, X. Cao, G. L. Wang, L. Wu, Z. S. Li, J. Solid State Electrochem, 2010, **14**, 851-855.

13. D. X. Cao, L. Wu, Y. Sun, G. L. Wang, Y. Z. Lv, J. Power Sources, 2008, **177**, 624-630.

14. Y. Z. Lv, Y. Xu, D. X. Cao, J. Power Sources, 2011, **196**, 8809-8814.

15. Y. Z. Lv, M. Liu, D. X. Cao, J. Power Sources, 2013, **239**, 265-268.

16. Y. Z. Lv, M. Liu, D. X. Cao, J. Power Sources, 2013, **225**, 124-128.

17. Y. B. Ma, N. Li, D. Y. Li, J. Power Sources, 2011, **196**, 2346-2350.

18. X. G. Meng, R. Z. Wu, M. L. Zhang, J. Alloys Compd, 2009, **486**, 722-725.

19. M. Anik, G. Celikten, J. Corros. Sci, 2007, **49**, 1878-1894.

20. G. Song, A. Atrens, X. Wu, et al, J. Corros. Sci, 1998, **40**, 1769 -1791.

Figure captions:

Fig. 1. The potentiodynamic polarization curves for the Mg-11Li-3.5Al-2Zn-1.5Re-0.5Zr electrode in 0.7 mol L^{-1} NaCl solution containing different concentrations of $C_6H_{12}N_4$ ((a) 0.00 mmol L^{-1}; (b) 0.05 mmol L^{-1}; (c) 0.10 mmol L^{-1}; (d) 0.50 mmol L^{-1}; (e) 0.80 mmol L^{-1}; (f) 1.00 mmol L^{-1}; (g) 2.00 mmol L^{-1}).

Fig. 2. The current-time curves measured at -0.8 V for the Mg-11Li-3.5Al-2Zn-1.5Re-0.5Zr electrode in 0.7 mol L^{-1} NaCl solution containing different concentrations of $C_6H_{12}N_4$ ((a) 0.00 mmol L^{-1}; (b) 0.05 mmol L^{-1}; (c) 0.10 mmol L^{-1}; (d) 0.50 mmol L^{-1}; (e) 0.80 mmol L^{-1}; (f) 1.00 mmol L^{-1}; (g) 2.00 mmol L^{-1}).

Fig. 3. The current-time curves measured at -1.0 V for the Mg-11Li-3.5Al-2Zn-1.5Re-0.5Zr electrode in 0.7 mol L^{-1} NaCl solution containing different concentrations of $C_6H_{12}N_4$ ((a) 0.00 mmol L^{-1}; (b) 0.05 mmol L^{-1}; (c) 0.10 mmol L^{-1}; (d) 0.50 mmol L^{-1}; (e) 0.80 mmol L^{-1}; (f) 1.00 mmol L^{-1}; (g) 2.00 mmol L^{-1}).

Fig. 4. The current-time curves measured at -1.2 V for the Mg-11Li-3.5Al-2Zn-1.5Re-0.5Zr electrode in 0.7 mol L^{-1} NaCl solution containing different concentrations of $C_6H_{12}N_4$ ((a) 0.00 mmol L^{-1}; (b) 0.05 mmol L^{-1}; (c) 0.10 mmol L^{-1}; (d) 0.50 mmol L^{-1}; (e) 0.80 mmol L^{-1}; (f) 1.00 mmol L^{-1}; (g) 2.00 mmol L^{-1}).

Fig. 5. The current-time curves measured at -1.4 V for the Mg-11Li-3.5Al-2Zn-1.5Re-0.5Zr electrode recorded in 0.7 mol L^{-1} NaCl solution containing different concentrations of $C_6H_{12}N_4$ ((a) 0.00 mmol L^{-1}; (b) 0.05 mmol L^{-1}; (c) 0.10 mmol L^{-1}; (d) 0.50 mmol L^{-1}; (e) 0.80 mmol L^{-1}; (f) 1.00 mmol L^{-1}; (g) 2.00 mmol L^{-1}).

Fig. 6. The impedance spectra for the Mg-11Li-3.5Al-2Zn-1.5Re-0.5Zr electrode recorded in (a)0.7 mol L^{-1} NaCl solution and (b) 0.7 mol L^{-1} NaCl solution containing 0.10 mmol L^{-1} $C_6H_{12}N_4$.

Fig. 7. The SEM micrographs of the Mg-11Li-3.5Al-2Zn-1.5Re-0.5Zr electrode obtained after its potentiostatic discharging at -1.0 V for 15 min in 0.7 mol L^{-1} NaCl solution containing different concentrations of $C_6H_{12}N_4$ ((a) 0.00 mmol L^{-1}; (b) 0.10 mmol L^{-1}; (c) 1.00 mmol L^{-1}).

Table captions:

Table 1 Chemical compositions of alloys (wt.%).

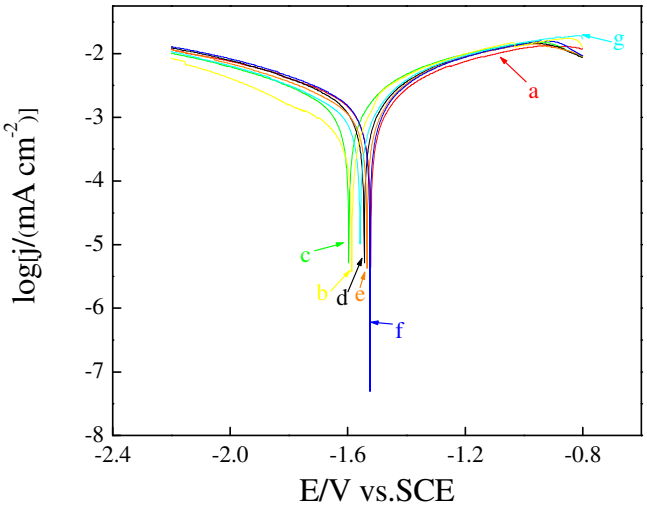

Fig.1. The potentiodynamic polarization curves for the Mg-11Li-3.5Al-2Zn-1.5Re-0.5Zr electrode in 0.7 mol L^{-1} NaCl solution containing different concentrations of $C_6H_{12}N_4$ ((a) 0.00 mmol L^{-1}; (b) 0.05 mmol L^{-1}; (c) 0.10 mmol L^{-1}; (d) 0.50 mmol L^{-1}; (e) 0.80 mmol L^{-1}; (f) 1.00 mmol L^{-1}; (g) 2.00 mmol L^{-1}).

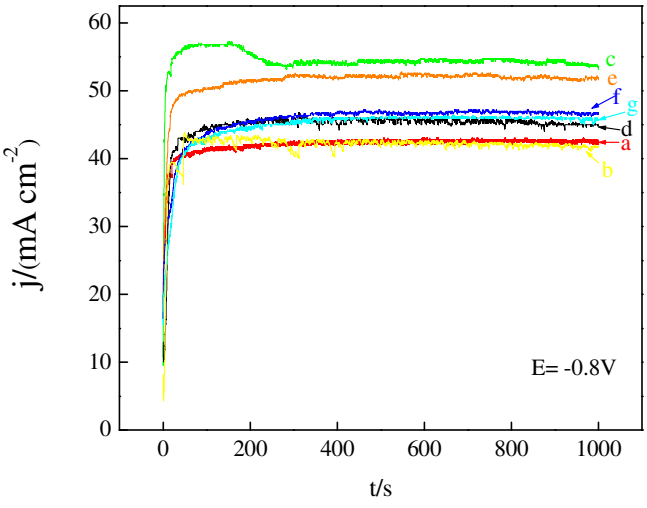

Fig.2. The current-time curves measured at -0.8 V for the

Mg-11Li-3.5Al-2Zn-1.5Re-0.5Zr electrode in 0.7 mol L^{-1} NaCl solution containing different concentrations of $C_6H_{12}N_4$ ((a) 0.00 mmol L^{-1};(b) 0.05 mmol L^{-1}; (c) 0.10 mmol L^{-1}; (d) 0.50 mmol L^{-1}; (e) 0.80 mmol L^{-1}; (f) 1.00 mmol L^{-1}; (g) 2.00 mmol L^{-1}).

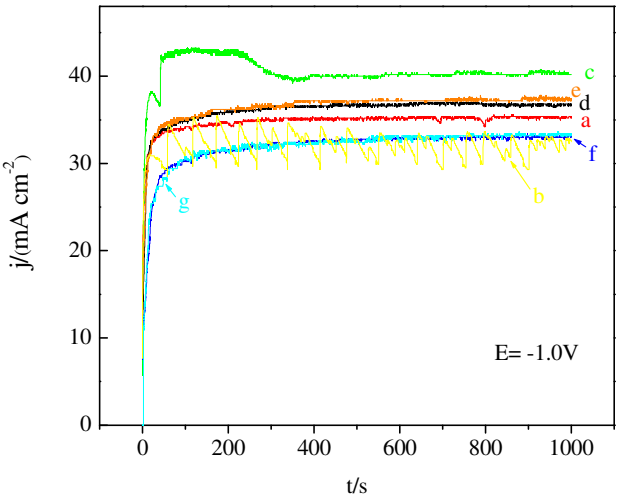

Fig. 3. The current-time curves measured at -1.0V for the Mg-11Li-3.5Al-2Zn-1.5Re-0.5Zr electrode in 0.7 mol L^{-1} NaCl solution containing different concentrations of $C_6H_{12}N_4$ ((a) 0.00 mmol L^{-1}; (b) 0.05 mmol L^{-1};(c) 0.10 mmol L^{-1}; (d) 0.50 mmol L^{-1}; (e) 0.80 mmol L^{-1}; (f) 1.00 mmol L^{-1}; (g) 2.00 mmol L^{-1}).

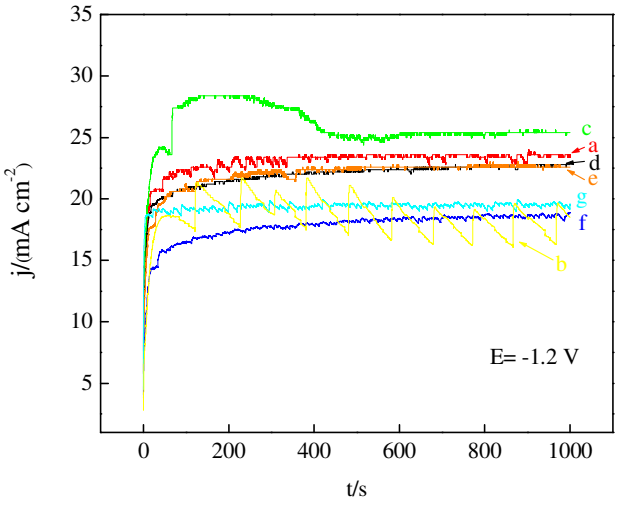

Fig.4. The current-time curves measured at -1.2 V for the Mg-11Li-3.5Al-2Zn-1.5Re-0.5Zr electrode in 0.7 mol L^{-1} NaCl solution containing different concentrations of $C_6H_{12}N_4$((a) 0.00 mmol L^{-1}; (b) 0.05 mmol L^{-1};(c) 0.10 mmol L^{-1}; (d) 0.50 mmol L^{-1}; (e) 0.80 mmol L^{-1}; (f) 1.00 mmol L^{-1}; (g) 2.00 mmol L^{-1}).

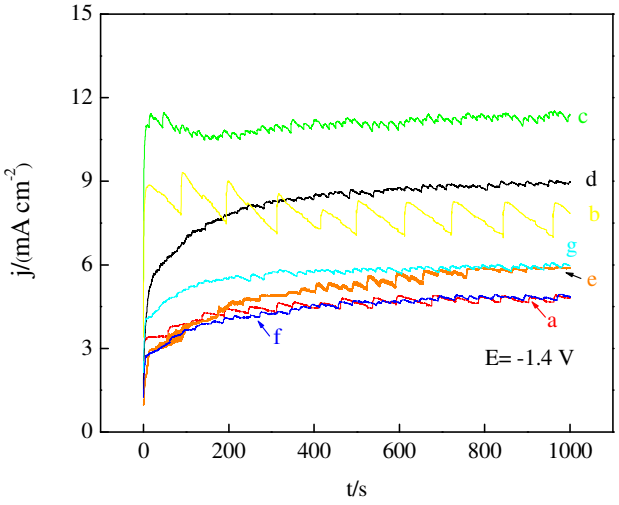

Fig.5. The current-time curves measured at -1.4 V for the Mg-11Li-3.5Al-2Zn-1.5Re-0.5Zr electrode recorded in 0.7 mol L^{-1} NaCl solution

containing different concentrations of $C_6H_{12}N_4$ ((a) 0.00 mmol L^{-1}; (b) 0.05 mmol L^{-1};(c) 0.10 mmol L^{-1}; (d) 0.50 mmol L^{-1}; (e) 0.80 mmol L^{-1}; (f) 1.00 mmol L^{-1}; (g) 2.00 mmol L^{-1}).

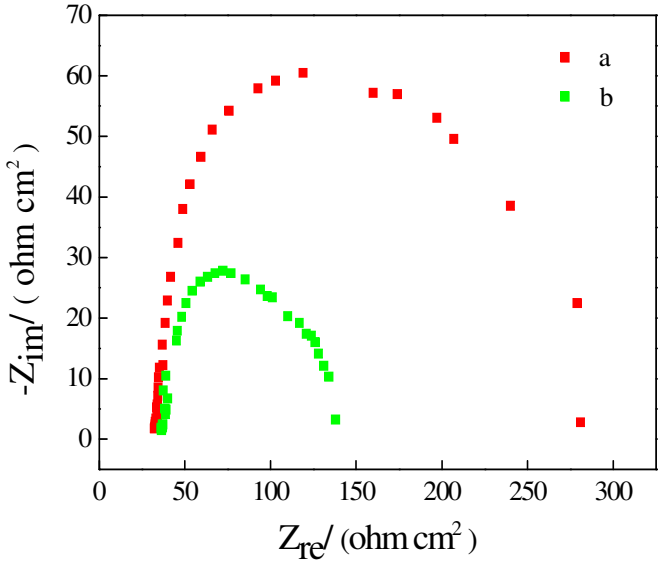

Fig.6. The impedance spectra for the Mg-11Li-3.5Al-2Zn-1.5Re-0.5Zr electrode recorded in (a) 0.7 mol L^{-1}NaCl solution and (b) 0.7 mol L^{-1}NaCl solution containing 0.10 mmol L^{-1} $C_6H_{12}N_4$.

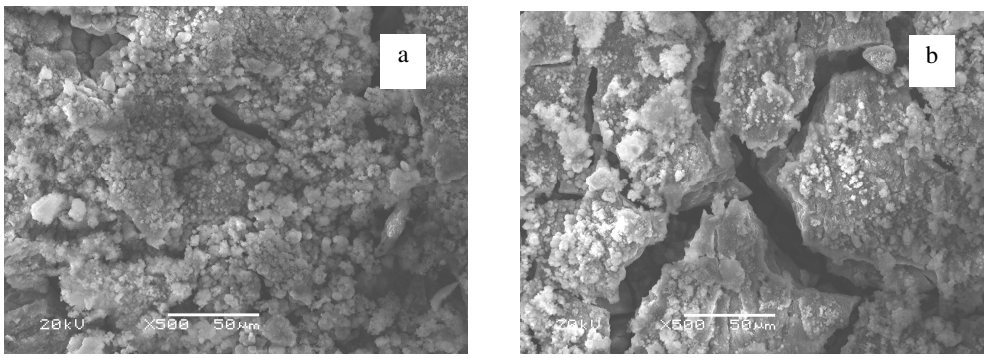

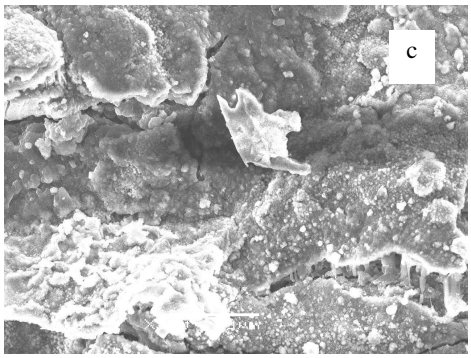

Fig. 7. The SEM micrographs of the Mg-11Li-3.5Al-2Zn-1.5Re-0.5Zr electrode obtained after its potentiostatic discharging at -1.0 V for 15 min in 0.7 mol L^{-1} NaCl solution containing different concentrations of $C_6H_{12}N_4$ ((a) 0.00 mmol L^{-1}; (b) 0.10 mmol L^{-1}; (c) 1.00 mmol L^{-1}).

Table

Table 1 Chemical compositions of alloys (wt.%).

Alloys	Mg	Li	Al	Zn	Re	Zr
Mg-11Li-3.5Al-2Zn-1.5R-0.5Zr	81.5	11	3.5	2	1.5	0.5